Sensorless Fuzzy Sliding Mode Speed Controller for Induction Motor with DTC based on Artificial Neural Networks

SARRA MASSOUM, ABDELKADER MEROUFEL, ABDERRAHIM BENTAALLAH, FATIMA ZOHRA BELAIMECHE, AHMED MASSOUM
Department of electrical engineering,
Faculty of Technologie,
Djillali Liabes University, Sidi Bel-Abbes,
ALGERIA
lalem_sarra@yahoo.fr

Abstract - The objective of this work is to develop a Fuzzy Sliding Mode Speed Controller and to replace the conventional selector switches of the voltage inverter by a selector based on Artificial Neural Networks (ANNs) for the induction motor drive. The Direct Torque Control (DTC) is known to produce quick and robust response in AC drive system. However, during steady state, torque, flux and current ripple occurs. An improvement of electric drive system can be obtained using a DTC method based on ANNs which reduces the torque and flux ripples. The rotor speed and stator flux are estimated by the model reference adaptive system (MRAS) scheme which is determined from measured terminal voltages and currents. The speed loop is carried out by a Fuzzy Sliding Mode Controller (FSMC) giving high performance and robustness to the drive system. The MATLAB SIMULINK is used to perform the simulation. The simulated results of this method are discussed and compared with conventional DTC.

Key- words: DTC, induction motor, MRAS, speed FSMC, ANNs, torque ripple minimization

1 Introduction

The robustness, the low cost, the performances and the ease of maintenance make the asynchronous motor advantageous in many industrial applications or general public. Recent advances in power semiconductor and microprocessor technology have made possible the application of advanced control techniques to alternating current (AC) motor drive systems. Direct Torque Control (DTC) has become a popular technique for the control of Induction Motor (IM) drives as it provides a fast dynamic torque response and is robust to machine parameter variations without the use of current regulators [1]. This technique can be implemented easily using two hysteresis controllers and a Switching Table (ST) to select the switching voltage vector. Although DTC has some drawbacks, such as the torque and flux ripple [2]**.** In recent years ANNs have gained a wide attention in control applications. For that, we developed an intelligent technique to improve the dynamic performances of the DTC. This method consists in replacing the traditional ST applied to the IM- DTC by an ANNs and the classical speed controller by a fuzzy sliding mode speed controller in order to achieve good robustness of IM drive [3],[4],[5]. The ANNs are capable of learning the desired mapping between the inputs and outputs signals of the system without knowing the exact mathematical model of the system. The ANNs are excellent estimators in non linear systems [6]. Various ANN based control strategies have been developed for DTC IM drive to overcome the scheme drawback [7],[8]. Fuzzy Logic Control (FLC) strategy based on human knowledge can cope with parameter uncertainties, imprecision and does not rely on any mathematical models [9]. The Sliding Mode Control (SMC) can offer many good properties, such as good performance against unmodelled dynamics, insensivity to parameter variations, external disturbance rejection and fast dynamic response [10]. Thus, the FSMC which combines the effects of FLC and SMC is applied to improve the speed response. The rotor speed is estimated by MRAS scheme which is determined from measured terminal voltages and currents. The speed estimator is then applied to sensorless DTC-ANNs of IM drive system. The FSMC is used in order to increase the performances and the robustness of the speed closed loop.

The modeling is presented in Matlab/Simulink models in order to study the performance of the drive system under steady state and dynamic conditions during starting, and speed reversal and load perturbations. The simulation results show that the proposed control method can achieve very robust and satisfactory performance.

2 Principle of DTC

The block diagram of classical DTC scheme is shown in figure 1.

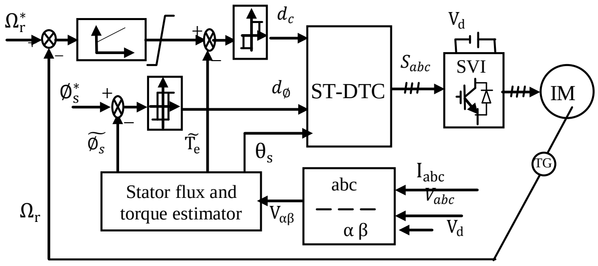

Fig.1. Block diagram of simulated ST-DTC with speed controller

The stator flux and torque magnitudes are controlled by two independent hysteresis controllers. The selection of the appropriate voltage vector is based on the switching table given in Table1.

Table 1. Basing Switching

$\emptyset_s$	C_e	$z1$	$z2$	$z3$	$z4$	$z5$	$z6$
$d_\emptyset = o$	$d_c = 1$	V_3	V_4	V_5	V_6	V_1	V_2
	$d_c = o$	V_0	V_7	V_0	V_7	V_0	V_7
	$d_c = -1$	V_5	V_6	V_1	V_2	V_3	V_4
$d_\emptyset = 1$	$d_c = 1$	V_2	V_3	V_4	V_5	V_6	V_1
	$d_c = o$	V_7	V_0	V_7	V_0	V_7	V_0
	$d_c = -1$	V_6	V_1	V_2	V_3	V_4	V_5

By using only current and voltage measurements, it is possible to estimate the instantaneous stator flux and output torque. The methods of DTC consist in controlling directly the opening or closing the inverter switches from the computed values of stator flux and torque. The state's changes of the switches are related to the evolution of the electromagnetic state of the motor.

PI controller is proposed for outer speed control loop to achieve swift response, less overshooting and precision speed control.

2.1 Stator flux control

Stator flux estimation based on voltage model is estimated by using equation:

$$\overline{\emptyset_s} = \int_0^t (\overline{V_s} - R_s \overline{I_s})dt \qquad (1)$$

During the switching interval, when stator resistance drop is neglected in high speed operating condition, the relationship between the voltage vectors and flux variation is given by

$$\overline{\emptyset}_s(k+1) \approx \overline{\emptyset}_s(k) + \overline{V}_s T_e \;\text{ or }\; \Delta\overline{\emptyset}_s(k) = \overline{V}_s T_e \quad . \qquad (2)$$

The instantaneous flux speed is only governed by voltage vector amplitude given in (2). The values of $\overline{V}_s$ and $\overline{I}_s$ are calculated by using the DC link voltage V_{dc}, the inverter switching states S_a, S_b, and S_c, and the motor line currents I_{abc}.

It can be proven that the space vector of the rotor flux is related to that of the stator flux by the following equation in the s-domain with a first-order delay equation.

$$\overline{\emptyset}_r = \frac{L_m}{L_s} \frac{\overline{\emptyset}_s}{1 + s\delta T_r} \qquad (3)$$

The stator flux angle is calculated by

$$\theta_s = \arctan\left(\frac{\emptyset_{qs}}{\emptyset_{ds}}\right) \overline{\emptyset}_r \qquad (4)$$

2.2 Electromagnétic torque control

The electromagnetic torque is proportional to the vector product between the stator and rotor flux vector:

$$T_e = \frac{3}{2} \frac{pM}{L_r L_s} (\emptyset_{ds} I_{qs} - \emptyset_{qs} I_{ds}) \qquad (5)$$

3 Rotor speed estimation by MRAS technique

Sensorless drives are becoming more and more important as they can eliminate the speed sensor maintaining accurate response. Monitoring only the stator current and stator voltages, it is possible to estimate the necessary control variables. The observer type used here is a MRAS [2]. The basic scheme of the MRAS configuration is given in figure 2. The scheme consists of two models; reference and adjustable ones and an adaptation mechanism. The block "reference model" represents voltage model which is independent of speed. The block "adjustable model" is the current model which is using speed as a parameter. The block "adaptation mechanism (PI controller)" estimates the unknown parameter using the error between the reference and the adjustable models and updates the adjustable model with the estimated parameter until satisfactory performance is achieved. Since the MRAS is a close-loop system, the accuracy can be increased. However, the models contain pure integrators which cause estimation error due to unknown initial condition and estimation drift due to offset in the measured currents. To avoid the problem, low-pass filters are used [2].

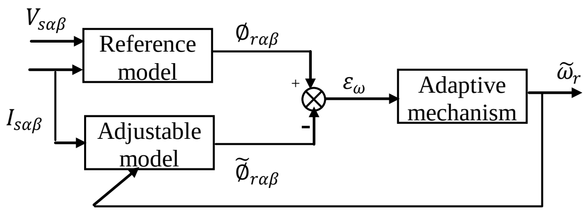

Fig.2. Classical MRAS structure for speed estimation

3.1 Reference model equation

The reference rotor flux components obtained from the reference model are given by:

$$[\emptyset_{r\alpha\beta}] = \frac{L_r}{L_m}\left(\int([V_{s\alpha\beta}] - R_s[I_{s\alpha\beta}])dt - \sigma L_s[I_{s\alpha\beta}]\right) \quad (6)$$

3.2 Adaptive model equation

The rotor flux components obtained from the adaptive model are given by:

$$[\tilde{\emptyset}_{r\alpha\beta}] = \int\left(\left(-\frac{1}{T_r} + \omega_r\right)[\tilde{\emptyset}_{r\alpha\beta}] + \frac{L_m}{T_r}[I_{s\alpha\beta}]\right)dt \quad (7)$$

3.3Error between two models

Finally the adaptation scheme generates the value of the estimated speed to be used in such a way as to minimize the error between the reference and estimated fluxes. In the classical rotor flux MRAS scheme, this is performed by defining a speed tuning signal ε_ω , to be minimized by a PI controller which generates the estimated speed which is fed back to the adaptive model. The expressions for the speed tuning signal and the estimated speed can be given as:

$$\varepsilon_\omega = (\emptyset_{r\beta}\tilde{\emptyset}_{r\alpha} - \emptyset_{r\alpha}\tilde{\emptyset}_{r\beta}) \quad (8)$$

$$\tilde{\omega}_r = k_p\varepsilon_\omega + k_i\int\varepsilon_\omega dt. \quad (9)$$

4 ANN based DTC

The neurons artificial network is a model of calculation with a conception schematically inspired by the real neurons functioning system. Formal units, once assembled, help to realize complex information processing. It constitutes an approach which gives more opportunities to approach the problems of perception, memory, learning and analysis under new angles. It is also a very promising alternative to avoid certain limitations of the classic numeric methods. Due to its parallel treatment of the information, it infers emergent properties able to resolve problems qualified in the past as complex. The back propagation algorithm is one of the most popular algorithms for training a network due to its success from both the simplicity and applicability viewpoint. The algorithm consists of two phases: the training phase and the recall phase. In the training phase, first, the weights of the network are randomly initialized. Then, the output of the network is calculated and compared to the desired value. Next, the error of the network is calculated and used to adjust the weights of the output layer. Similarly, the network error is also propagated backwards and used to update the weights of the previous layers. In this article, the table of commutation is replaced by an artificial network of neurons figure 3.

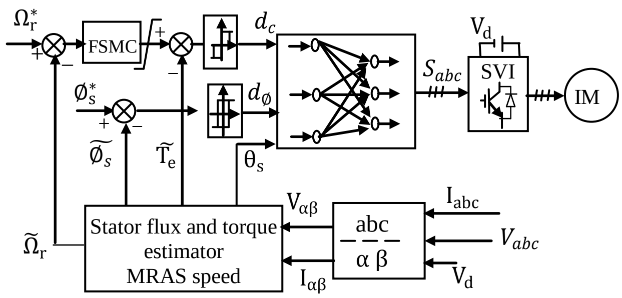

Fig.3. Block diagram of simulated direct torque neural networks control with MRAS for speed FSMC

The neural network selector inputs proposed are the position of flux stator vector represented by the number of the corresponding sector, the error between its estimated value and the reference value and the difference between the estimated electromagnetic torque and the torque reference that is to say three neurons of the input layer. The output layer is composed of three neurons, each representing the state S_{abc} of one of the three pairs of switches of the inverter connected to the positive DC bus. After several tests we take an architecture 3-9-3 with a single hidden layer. The function activation of the hidden layer is Tansig while the activation function of the output layer is Purelin. The learning of the neural network is done by using the algorithm levenberg Marquardt with a number of epochs 500 and an error of 10^{-3}.

5 Fuzzy sliding mode control

FSMC is at present employed as an alternative to develop controller for systems that cannot be precisely modelled and whose parameters vary [8]. To design a sliding mode speed controller for IM DTC drive, consider the mechanical equation:

$$\frac{J}{p}\dot{\omega_r} + \frac{K_f}{p}\omega_r + T_r = T_e. \tag{10}$$

Where ω_r is the rotor speed in electrical rad/s, rearranging to get:

$$\dot{\omega_r} = \frac{p}{J}T_e - \frac{K_f}{J}\omega_r - \frac{p}{J}T_r \tag{11}$$

Considering Δa and Δb as bounded uncertainties introduced by system parameters J and K_f, (11) can be rewritten as [11]:

$$\dot{\omega} = (a + \Delta a)\omega_r + (b + \Delta b)T_e + cT_r \tag{12}$$

Where: $a = -\frac{K_f}{J}$, $b = \frac{p}{J}$,$c = -\frac{p}{J}$

Defining the state variable of the speed error as:

$$e(t) = \omega_r(t) - \omega_r^*(t) \tag{13}$$

Combining (12) with (13) and taking the derivative of (13) yields

$$\dot{e(t)} = ae(t) + b\{T_e + d(t)\} \tag{14}$$

Where d(t) is the lumped uncertainty defined as:

$$d(t) = \frac{\Delta a}{b}\omega_r(t) + \frac{\Delta b}{b}T_e + \frac{c}{b}T_r \tag{15}$$

And

$$\overline{T_e} = T_e(t) + \frac{a}{b}\omega_r^* \tag{16}$$

Defining a switching surface $s(t)$ from the nominal values of system parameters a and b [11]:

$$s(t) = e(t) - \int_0^t (a + bk)e(\tau)d\tau \tag{17}$$

Such that the error dynamics at the sliding surface $s(t) = \dot{s}(t) = 0$ will be forced to exponentially decay to zero, then the error dynamics can be described by:

$$\dot{e}(t) = (a + bk)e(t) \tag{18}$$

where k is a linear negative feedback gain [11]. A speed control law can be defined as:

$$\overline{T_e} = ke(t) - \beta sign(s(t)) \tag{19}$$

where β is known as hitting control gain used to make the sliding mode condition possible and the sign function can be defined as [11]:

$$sign(s) = \begin{cases} 1 & \text{if } s > 0 \\ 0 & \text{if } s = 0 \\ -1 & \text{if } s < 0 \end{cases} \tag{20}$$

The final electromagnetic torque command T_e^* of the output of the sliding mode speed controller can be obtained by directly substituting (16) into (19). Basically, the control law for T_e^* is divided into two parts: equivalent control U_{eq} which defines the control action when the system is on the sliding mode and switching part U_s which ensures the existence condition of the sliding mode. If the friction B is neglected expressions for U_{eq} and U_s can be written as:

$$\begin{cases} U_{eq} = ke(t) \\ U_s = -\beta sign(s(t)) \end{cases} \tag{21}$$

To guarantee the existence of the switching surface consider a Lyapunov function [6]:

$$V(t) = \frac{1}{2}s^2(t) \tag{22}$$

Based on Lyapunov theory, if the function $\dot{V}(t)$ is negative definite, this will ensure that the system trajectory will be driven and attracted toward the sliding surface s(t) and once reached, it will remain sliding on it until the origin is reached asymptotically [11]. Taking the derivative of (22) and substituting from the derivative of (17):

$$\dot{V}(t) = s(t)\dot{s}(t) = s(t)\{\dot{e}(t) - (a + bk)e(t)\} \tag{23}$$

Substitute from (14) into (23):

$$s(t)\dot{s}(t) = s(t)\{b\overline{T}_e(t) + bd(t) - bke(t)\} \quad (24)$$

Using (19) gives:

$$s(t)\dot{s}(t) = s(t)\{-\beta sign(s(t)) - d(t)\} \quad (25)$$

To ensure that (25) will be always negative definite, the value of the hitting control gain β should be designed as the upper bound of the lumped uncertainties d(t), i.e.

$$\beta \geq |d(t)| \quad (26)$$

However, it is difficult practically to estimate the bound of uncertainties in (15). Therefore the hitting control gain β has to be chosen large enough to overcome the effect of any external disturbance [8], [11]. Therefore the speed control law defined in (19) will guarantee the existence of the switching surface s(t) in (17) and when the error function e(t) reaches the sliding surface, the system dynamics will be governed by (18) which is always stable [11]. Moreover, the control system will be insensitive to the uncertainties Δa , Δb and the load disturbance C_r [8], [11]. The use of the sign function in the sliding mode control (19) will cause high frequency chattering due to the discontinuous control action which represents a severe problem when the system state is close to the sliding surface [8]. To overcome this problem an approach which combines FL with SM is used [8], [11]. The saturation function is replaced by a fuzzy inference system in order to avoid the chattering phenomenon. The FSMC is a single input single output fuzzy logic controller. It is constructed from the following format 'IF….THEN' rules or equivalently. The max-min composition is chosen as the inference method. The crisp output is obtained by the center of the area defuzzifier. The If-Then rules of the fuzzy logic controller can be written as [11]:

If s is NB then U_s is BIGGER
If s is NM then U_s is BIG
If s is Z then U_s is MEDIUM
If s is PM then U_s is SMALL
If s is PB then U_s is SMALLER

The proposed controller uses following linguistic labels: {NB Negative Big), NM Negative Medium), Z (Zero), PM (Positive Medium), PB (Positive Big)}. Each fuzzy label has an associated membership function.

The membership functions for the input and output (figure 4) of the FL controller have a triangular and trapezoidal form and are obtained by trial error to ensure optimal performance.

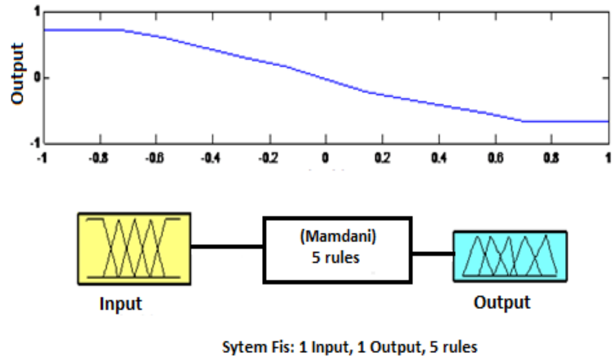

Fig.4. Fuzzy sliding mode switching and fuzzy logic membership functions DSIM Slinding

6 Simulation results and discussions

The proposed scheme has been implemented with Matlab/Simulink in order to evaluate its performances. The IM used for the simulations has the following parameters:

Nominal voltage : 220 / 380 V,
Nominal current : 6.4 / 3.7 A
Nominal power: 1.5 kW
A number of pairs of poles: p = 2
Stator resistance by phase : $R_s = 4.85\Omega$
Rotor resistance by phase : $R_r = 3.805\Omega$
stator inductance: $L_s = 0.274$ H
Rotor inductance : $L_r = 0.274$ H
Mutual inductance : $L_m = 0.258$ H
Moment of inertia: J= $0.031\ kg.m^2$
Nominal speed: N = 1420 tr /min
Coefficient of friction: $f_r = 0.000114\ Nm.s^{-1}/rd$

Figure 5 shows classical DTC command where the references are the torque reverse from +10Nm to -10Nm and the stator flux 1.2Wb.

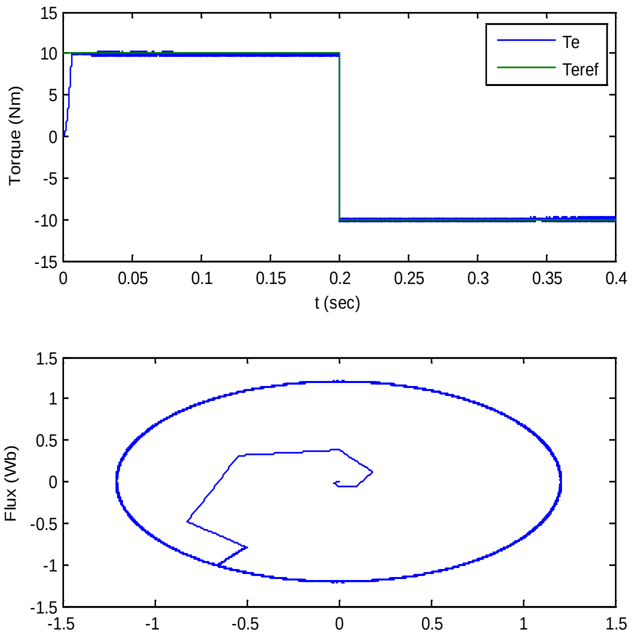

Fig.5. Classical responses ST-DTC

It is clear that the electromagnetic torque (T_e) follows the torque reference T_{eref} rapidly and exactly. In spite of the torque control abrupt change, the stator flux maintains the form circular what shows decoupling between the couple and stator flux

Figure 6 shows the simulation results for the ST-DTC-IM under classical PI speed controller. The speed tracking to the reference, the decoupling between torque and stator flux and disturb rejection was verified.

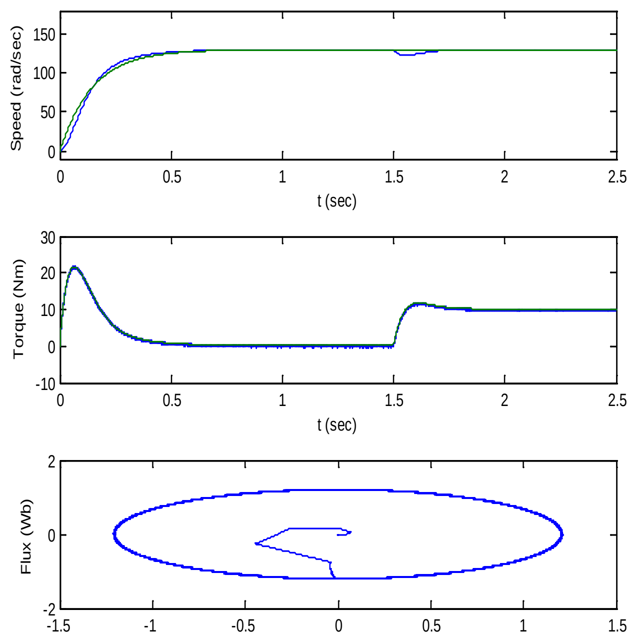

Fig. 6. Response of the system based on speed PI controller for ST-DTC

Figure 7 Shows ANN-DTC command where the references are the torque reverse from +10Nm to -10Nm and the stator flux 1.2Wb

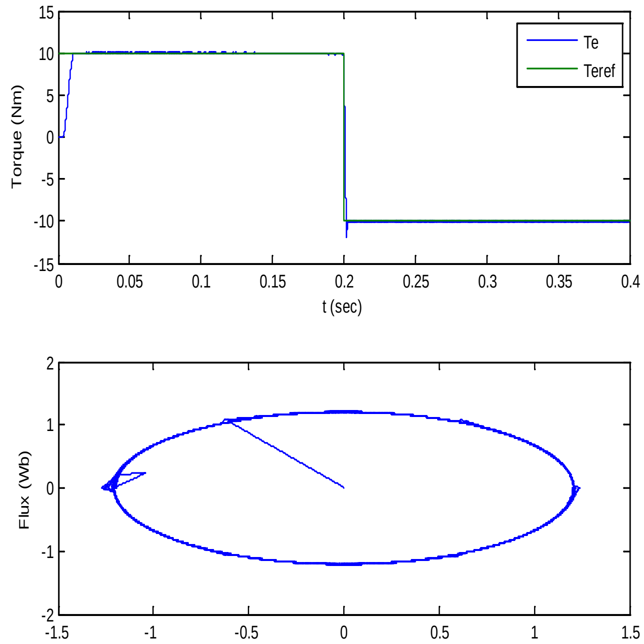

Fig.7. ANN-DTC responses

The simulation results obtained in the test below are conducted on the behavior of the proposed MRAS speed estimator and shown in figure 8.

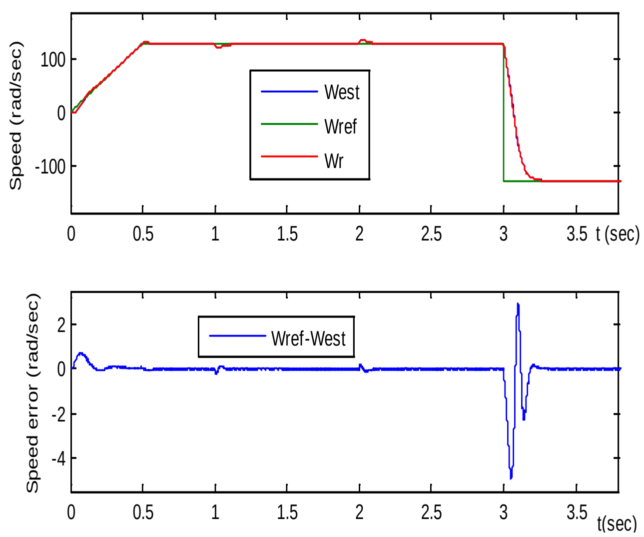

Fig.8. Simulation results of speed estimator (West), reference speed (Wref) and rotor speed (Wr). Down speed error between reference and estimator speed

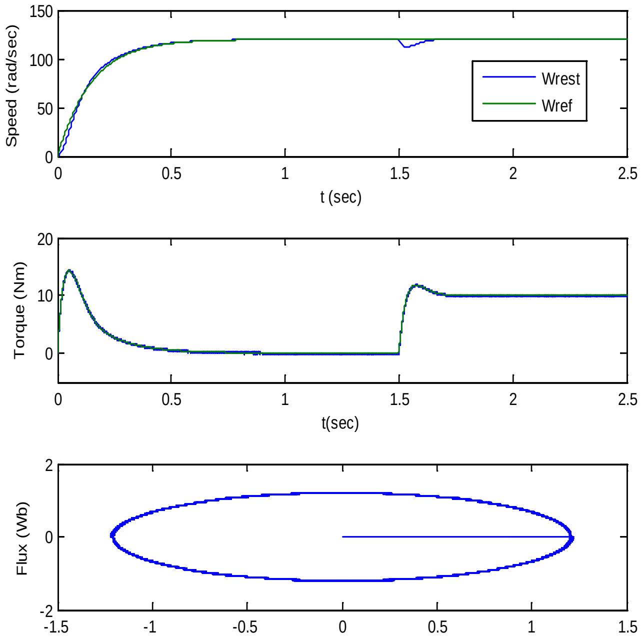

Fig.9. Response of the system based on speed PI controller for ANN- DTC

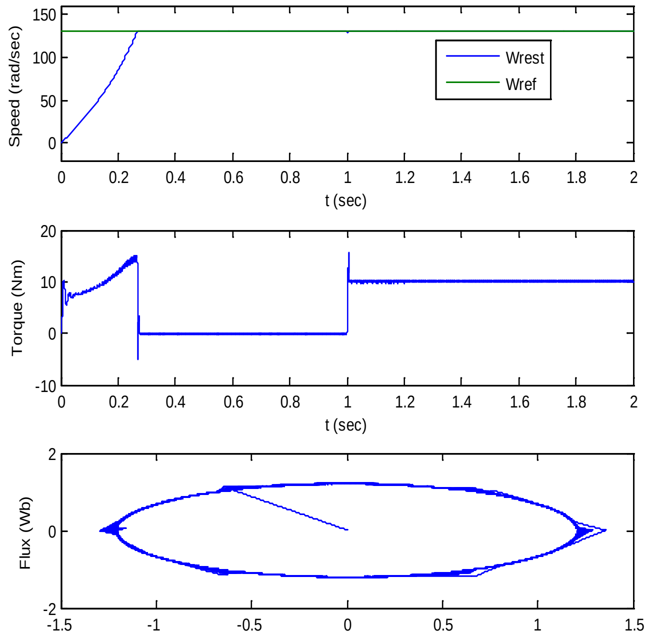

Fig.10. Response of the system based on speed FSMController for ANN-DTC

The proposed speed estimator guarantees good rotor speed tracking

The error shows well the estimated speed follow-up to the reference in spite of the abrupt command change

From this analysis, the torque and flux present a high dynamic performances and good precision in steady state. It can be observed that the torque and flux are decoupled. The torque and the flux ripples are due to the hysteresis-band comparator. From Figure 6 and Figure 9, we remark the same performances in both cases of DTC.

In order to improve the performances and robustness of the system, we replace the PI speed controller by a FSMC and we obtain the results in figure 9.

The command input is step reference for speed and the system is loaded at 1s with 10Nm. It can be seen that the speed response present a good performances (quick response with no overshoot, zero steady state error and good tracking reference speed). The external disturbance (load torque) on the speed response is rejected instantaneously. Better decoupled properties are obtained and flux tracks the desired flux precisely.

- Robustness tests

In order to test robustness of the proposed control, we have studied stator resistance and inertia variations.

- *Stator resistance variation*

The sensitivity of stator resistance is investigated because its variation greatly affects the performance of the DTC drive.

FSMC shows the robustness of the controller under the stator resistance variation and the load torque disturbance.

- *Inertia variation*

Another test is performed by applying step change in speed command with inertia variation. Figure 12 shows the behavior of the drive when inertia is increased 100% of its nominal value.

It is shown from figure 11 that the proposed drive can follow the reference speed accurately due to the robustness of the FSMC. We remark that the time speed response increases with inertia and the other performances are maintained.

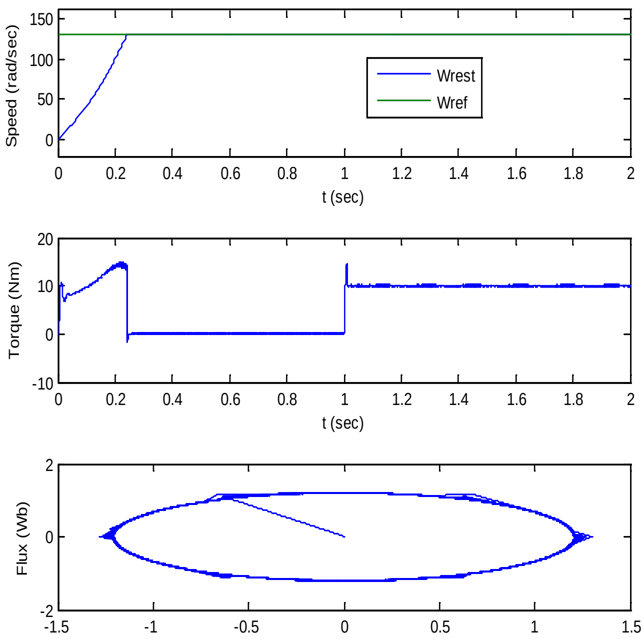

Fig.11. Speed, torque and stator flux responses with stator resistance $R_s = 2R_{sn}$ under FSMC

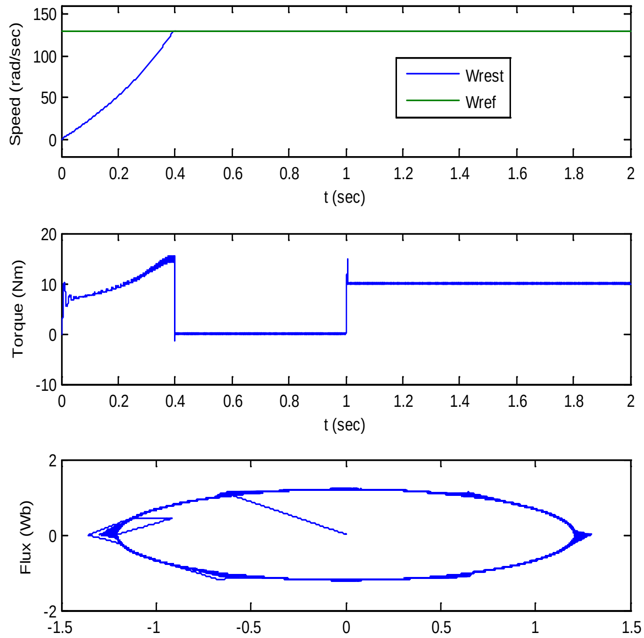

Fig.12. Speed, torque and flux responses with rotor inertia J=2*Jn

- *Ripple reduction*

The influence of chattering is investigated through a comparison between PI-classical-DTC, PI-ANN-DTC and FSMC- ANN-DTC (figure.13).

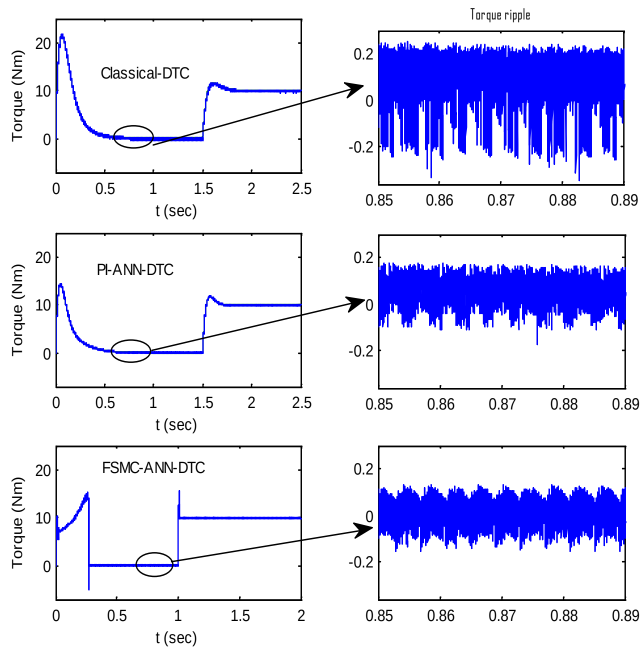

Fig.13. Torque response with zoom in steady state

From the analysis of these results, we establish the following remark. The amplitude of the torque ripples in steady state is gradually reduced.

7 Conclusion

From simulation results it was shown that the proposed FSMC for ANN-DTC is robust to external variations and has presented satisfactory performances in speed response (no overshoot, zero steady state error and good tracking reference speed). The robustness test has shown that it is insensitive to rotor resistance variation. The decoupling between the flux and the torque (speed) is maintained with regard to parameter variations and external load disturbance. The chattering phenomenon is decreased in torque when compared to PI-ANN-DTC. The FSMC-ANN-DTC has very interesting dynamic performances and provides improvement in ripple reduction in torque, so a lower harmonic content in the stator currents. With reduced torque fluctuations, current harmonics, vibrations, noise and hot in the motor are also reduced.

References:

[1] I.Takahashi, N.Toshihiko, A New Quick-Response and High-Efficiency Control Strategy of an Induction Motor, *IEEE Transactions on Industry Applications*, vol. IA-22, pp.820–827, September 1986.

[2] B. Robyns, F. Berthereau, J.-P. Hautier, H. Buyse , A fuzzy-logic-based multimodel field orientation in an indirect FOC of an induction motor, *IEEE Trans. on Industrial Electronics*, vol. 47, no. 2, pp. 380–388,April 2000.
[3] A. Meroufel, A. Massoum, and P. Wira, A Fuzzy Sliding Mode Controller for a Vector Controlled Induction Motor, *Industrial Electronics, ISIE 2008. IEEE International Symposium on ,* June 30 2008-July 2 2008, pp.1873–1878.
[4] S. M. Gadoue, D. Giaouris, and J.W. Finch, Genetic Algorithm Optimized PI and Fuzzy Sliding Mode Speed Control for DTC Drives, *Proceedings of the World Congress on Engineering* 2007, vol. I, London, U.K, WCE 2007, July 2 - 4, 2007.
[5] R. Kumar, S. V. Radmanaban, AnArtificial Neural Network Based Rotor Position Estimation for Sensorless Permanent Magnet Brushless DC Motor Drive, *IEEE conference.* (IECON-2006), Nov. 2006, pp.649–654.
[6] S. Jabeur, C.B, F. Fnaiech, DTFC and DTNFC: Two Intelligent Techniques for Induction Motors Torque Control, *Industrial Electronics, Proceedings of the IEEE International Symposium*, June 20-23 2005, pp: 131–138.
[7] L. M. Gnesiak, B. Ufnalski, Neural Stator Flux Estimator with Dynamical Signal Preprocessing, *IEEE Conf*erence. (AFRICON- 2004), pp. 1137–1142.
[8] F. Barrero, A. Gonzalez, A. Torralba, E. Galvan, L.G. Franquelo, Speed control of induction motors using a novel fuzzy sliding mode structure, *IEEE Trans. Fuzzy Syst,* vol.10,pp. 375–383, June 2002.
[9] V.I. UTKIN, Sliding mode control design principles and applications to electric drives, *IEEE Transactions on Industrial Electronics.*, vol.40, pp. 26–36, 1993